BINP-95-02
UCD-95-33
ISU-HET-95-5
October 1995

Study of Anomalous Couplings at a 500 GeV e^+e^- Linear Collider with Polarized Beams

A. A. Likhoded[(a)], T. Han[(b)] and G. Valencia[(c)]

[(a)] *On leave of absence from the Branch of The Institute for Nuclear Physics, Protvino, 142284 Russia.* E-mail: likhoded@mx.ihep.su

[(b)] *Department of Physics, University of California at Davis, Davis CA 95616*
E-mail: than@ucdhep.ucdavis.edu

[(c)] *Department of Physics, Iowa State University, Ames IA 50011*
E-mail: valencia@iastate.edu

Abstract

We consider the possibility of observing deviations from the Standard Model gauge-boson self-couplings at a future 500 GeV e^+e^- linear collider. We concentrate on the case in which the electroweak symmetry breaking sector is strongly interacting and there are no new resonances within reach of the collider. We find a sensitivity to the anomalous couplings that is two orders of magnitude higher than that achievable at LEP II. We also show how a polarized electron beam extends the reach of the collider, allowing experiments to probe different directions in parameter space.

1 Introduction

The Standard Model of electroweak interactions is in remarkable agreement with all precision measurements performed thus far [1]. These measurements, however, have not probed directly energy scales higher than a few hundred GeV, and precise measurements have been limited to scales up to the Z-mass. This has been used as a motivation to propose tests of the Standard Model by studying the self-couplings of the electroweak gauge bosons in future colliders.

Deviations from the self-couplings predicted by the minimal Standard Model are called "anomalous" gauge boson couplings and have been studied extensively in recent years. In particular, they have been discussed in the context of future e^+e^- colliders by many authors [2, 3]. There are two main differences between our present study and those that can be found in the literature. We interpret the success of the Standard Model as an indication that the $SU(2)_L \times U(1)_Y$ gauge theory of electroweak interactions is essentially correct, and that the only sector of the theory that has not been probed experimentally is the electroweak symmetry breaking sector. This point of view has many practical consequences in limiting the number of anomalous couplings that need to be studied, and in estimating their possible magnitude [4]. A second difference with other studies, is that we consider the effect of having polarized beams.

This paper is organized as follows. In Section 2 we summarize the effective Lagrangian formalism that we use to describe the anomalous couplings. In Section 3 we apply these results to a 500 GeV linear collider with polarized beams and discuss the relevant phenomenology. Finally we present our conclusions.

2 Anomalous Couplings for a Strongly-Interacting Electroweak Symmetry Breaking Sector

We wish to describe the electroweak symmetry breaking sector in the case in which there is no light Higgs boson or any other new particle. To do this in a model independent manner we use an effective Lagrangian for the interactions of gauge bosons of an $SU(2)_L \times U(1)_Y$ gauge symmetry spontaneously broken to $U(1)_Q$. The lowest order effective Lagrangian contains a gauge invariant mass term as well as the kinetic terms for the $SU(2)_L$ and $U(1)_Y$ gauge bosons [5]:

$$\mathcal{L}^{(2)} = \frac{v^2}{4}\mathrm{Tr}\Big(D^\mu \Sigma^\dagger D_\mu \Sigma\Big) - \frac{1}{2}\mathrm{Tr}\Big(W^{\mu\nu}W_{\mu\nu}\Big) - \frac{1}{2}\mathrm{Tr}\Big(B^{\mu\nu}B_{\mu\nu}\Big)\,. \tag{1}$$

$W_{\mu\nu}$ and $B_{\mu\nu}$ are the $SU(2)_L$ and $U(1)_Y$ field strength tensors

$$\begin{aligned} W_{\mu\nu} &= \frac{1}{2}\Big(\partial_\mu W_\nu - \partial_\nu W_\mu + \frac{i}{2}g[W_\mu, W_\nu]\Big)\,, \\ B_{\mu\nu} &= \frac{1}{2}\Big(\partial_\mu B_\nu - \partial_\nu B_\mu\Big)\tau_3\,, \end{aligned} \tag{2}$$

and $W_\mu \equiv W^i_\mu \tau_i$. The Pauli matrices τ_i are normalized so that $Tr(\tau_i \tau_j) = 2\delta_{ij}$.

The matrix $\Sigma \equiv \exp(i\vec{\omega}\cdot\vec{\tau}/v)$ contains the would-be Goldstone bosons ω_i that give the W and Z their mass via the Higgs mechanism, and the $SU(2)_L \times U(1)_Y$ covariant derivative is given by:

$$D_\mu \Sigma = \partial_\mu \Sigma + \frac{i}{2} g W^i_\mu \tau^i \Sigma - \frac{i}{2} g' B_\mu \Sigma \tau_3 \, . \tag{3}$$

The physical masses are obtained with $v \approx 246$ GeV. This non-linear realization of the symmetry breaking sector is a non-renormalizable theory that is interpreted as an effective field theory, valid below some scale $\Lambda \leq 3$ TeV. The lowest order interactions between the gauge bosons and fermions are the same as those in the minimal Standard Model.

Deviations from these minimal couplings (referred to as anomalous gauge boson couplings), correspond to higher dimension ($SU(2)_L \times U(1)_Y$ gauge invariant) operators. For energies below the scale of symmetry breaking Λ, it is possible to organize the effective Lagrangian in a way that corresponds to an expansion of scattering amplitudes in powers of E^2/Λ^2. The next to leading order effective Lagrangian that arises in this context has been discussed at length in the literature [5, 6, 7, 4, 8]. The contributions of this Lagrangian to the anomalous couplings have also been written down before [8].

In this paper we consider the process $e^+e^- \to W^+W^-$ at tree level and work in unitary gauge, therefore, the anomalous couplings enter the calculation only through the three gauge boson vertex VW^+W^- (where $V = Z, \gamma$).[1] It is conventional to write the most general CP conserving VW^+W^- vertex in the form [9]:

$$\begin{aligned}
\mathcal{L}_{WWV} \;=\; & -ie\frac{c_\theta}{s_\theta} g_1^Z \Big(W^\dagger_{\mu\nu} W^\mu - W_{\mu\nu} W^{\mu\,\dagger} \Big) Z^\nu - ie g_1^\gamma \Big(W^\dagger_{\mu\nu} W^\mu - W_{\mu\nu} W^{\mu\,\dagger} \Big) A^\nu \\
& -ie\frac{c_\theta}{s_\theta} \kappa_Z W^\dagger_\mu W_\nu Z^{\mu\nu} - ie\kappa_\gamma W^\dagger_\mu W_\nu A^{\mu\nu} \\
& -e\frac{c_\theta}{s_\theta} g_5^Z \epsilon^{\alpha\beta\mu\nu} \Big(W^-_\nu \partial_\alpha W^+_\beta - W^+_\beta \partial_\alpha W^-_\nu \Big) Z_\mu \, .
\end{aligned} \tag{4}$$

where $s_\theta = \sin\theta_W, c_\theta = \cos\theta_W$. The effective Lagrangian framework for the case of a strongly interacting symmetry breaking sector, predicts the five constants in Eq. (4), they are [8, 10]:

$$\begin{aligned}
g_1^Z &= 1 + \frac{e^2}{c_\theta^2} \Big(\frac{1}{2s_\theta^2} L_{9L} + \frac{1}{(c_\theta^2 - s_\theta^2)} L_{10} \Big) \frac{v^2}{\Lambda^2} + \cdots \, , \\
g_1^\gamma &= 1 + \cdots \, , \\
\kappa_Z &= 1 + e^2 \Big(\frac{1}{2 s_\theta^2 c_\theta^2} \Big(L_{9L} c_\theta^2 - L_{9R} s_\theta^2 \Big) + \frac{2}{(c_\theta^2 - s_\theta^2)} L_{10} \Big) \frac{v^2}{\Lambda^2} + \cdots \, ,
\end{aligned} \tag{5}$$

[1] The anomalous couplings also affect the $e\nu W$ and e^+e^-Z vertices through renormalization. However, they do so only through the parameter L_{10}, and we will argue later that it is not necessary to consider this coupling in detail because it has already been severely constrained at LEP.

$$\kappa_\gamma = 1 + \frac{e^2}{s_\theta^2}\Big(\frac{L_{9L}+L_{9R}}{2} - L_{10}\Big)\frac{v^2}{\Lambda^2} + \cdots ,$$
$$g_5^Z = \frac{e^2}{s_\theta^2 c_\theta^2}\hat{\alpha}\frac{v^2}{\Lambda^2} + \cdots .$$

In Eq. (5) we have written down the leading contribution to each anomalous coupling,[2] and denoted by $\cdots$ other contributions that arise at higher order ($\mathcal{O}(1/\Lambda^4)$), or at order $\mathcal{O}(1/\Lambda^2)$ with custodial $SU(2)$ breaking. We are thus assuming that whatever breaks electroweak symmetry has at least an approximate custodial symmetry. Under these assumptions there are only four operators in the next to leading order effective Lagrangian that are relevant:

$$\begin{aligned}\mathcal{L}^{(4)} &= \frac{v^2}{\Lambda^2}\Big\{-igL_{9L}\,\mathrm{Tr}\Big(W^{\mu\nu}D_\mu\Sigma D_\nu\Sigma^\dagger\Big) - ig'L_{9R}\,\mathrm{Tr}\Big(B^{\mu\nu}D_\mu\Sigma^\dagger D_\nu\Sigma\Big) \\ &+ gg'L_{10}\,\mathrm{Tr}\Big(\Sigma B^{\mu\nu}\Sigma^\dagger W_{\mu\nu}\Big) + g\hat{\alpha}\epsilon^{\alpha\beta\mu\nu}\mathrm{Tr}\Big(\tau_3\Sigma^\dagger D_\mu\Sigma\Big)\mathrm{Tr}\Big(W_{\alpha\beta}D_\nu\Sigma\Sigma^\dagger\Big)\Big\} \quad (6)\end{aligned}$$

The first three terms conserve the custodial $SU(2)_C$ symmetry, and we have explicitly introduced the factor v^2/Λ^2 in our definition of $\mathcal{L}^{(4)}$ so that the L_i are naturally of $\mathcal{O}(1)$. The term with $\hat{\alpha}$ breaks the custodial symmetry but we include it because it provides the leading contribution to g_5^Z. In theories with a custodial symmetry, this term is, therefore, expected to be smaller than the other ones in Eq. (6). This term is also special in that it is the only one at $\mathcal{O}(1/\Lambda^2)$ that violates parity while conserving CP. With our normalization, we expect $\hat{\alpha}$ to be of $\mathcal{O}(1)$ in theories without a custodial symmetry and much smaller in theories that have a custodial symmetry [11].

For our discussion we will assume that the new physics is such that the tree-level coefficients of $\mathcal{L}^{(4)}$ are larger than the (formally of the same order) effects induced by $\mathcal{L}^{(2)}$ at one-loop. More precisely, that after using dimensional regularization and a renormalization scheme similar to the one used in Ref. [4], the $L_i(\mu)$ evaluated at a typical scale (around 500 GeV for this process) are equal to the tree-level coefficients, and that their scale dependence is unimportant for the energies of interest. The physical motivation for this assumption is that, even if we do not see any new resonances directly, the effects of the new physics from high mass scales must clearly stand out if there is to be any hope of observing them. When the indirect effects of the new physics enter at the level of SM radiative corrections, very precise experiments (as the ones being performed at LEP I) are needed to unravel them. We are assuming that there will not be any such precision measurements in the next generation of high energy colliders.

All the necessary Feynman rules in unitary gauge have been written down in Ref. [10]. For our numerical study we will use the input parameters:

$$M_Z = 91.187\ \mathrm{GeV},\ \ \alpha = 1/128.8\,,\ \ G_F = 1.166\cdot 10^{-5}\ \mathrm{GeV}^{-2}\,. \quad (7)$$

[2]This is why we do not have terms corresponding to the usual λ_Z and λ_γ: they only occur at higher order in $1/\Lambda^2$.

We will also use $\Lambda = 2$ TeV as the scale normalizing our next to leading order effective Lagrangian, Eq. (6).

The parameter L_{10} can be very tightly constrained by precision measurements at LEP I [12]:

$$-1.1 \leq L_{10}(M_Z) \leq 1.5\,. \tag{8}$$

We find that this bound cannot be significantly improved with a 500 GeV linear collider so we will not study L_{10} further in this paper.

To summarize, we consider the next to leading order effective Lagrangian for a CP conserving, strongly interacting, electroweak symmetry breaking sector with an (at least) approximate custodial symmetry. We then find that the leading contribution to the anomalous couplings relevant for $e^+e^- \to W^+W^-$ at $\sqrt{s} = 500$ GeV can be written down in terms of four coupling constants. Finally we note that one of those coupling constants has already been tightly constrained at LEP I. We are thus left with a model that contains only three parameters L_{9L}, L_{9R}, and $\hat{\alpha}$. In the following sections we discuss the phenomenology of these three constants at a future linear collider with polarized beams.

3 Bounds from the process $e^+e^- \to W^+W^-$

The process of W-boson pair production in e^+e^- collisions in the Born approximation is determined by the diagrams shown in Fig. 1. The full circles represent vertices that include both the standard model couplings, and the anomalous couplings. The anomalous couplings enter these vertices directly or through renormalization of standard model parameters [10]. We will denote the degree of longitudinal polarization of the electron and positron by z_1 and z_2, respectively. Our notation is such that $z_1 = 1$ corresponds to a *right-handed* electron, whereas $z_2 = 1$ corresponds to a *left-handed* positron. The cross section for $e^+e^- \to W^+W^-$ with polarized beams can be written in terms of the usual Mandelstam variables s and t as:

$$\begin{aligned}\int_{t_{min}}^{t_{max}} \frac{d\sigma}{dt} dt &= \frac{\pi\alpha^2}{4s^2 M_W^4} \\ &\cdot \sum_{i,j=1}^{3} C_{ij}\left(T_{ij}(t_{max}) - T_{ij}(t_{min})\right)\,. \end{aligned} \tag{9}$$

The terms $C_{ij}T_{ij}$ give the contributions of the pair products of amplitudes of the corresponding diagrams (see Fig. 1) to the cross-section. The coefficients C_{ij} depend on the electroweak parameters and on the polarization of the initial particles. They are:

$$\begin{aligned} C_{11} &= \frac{S_1}{s^2}, \\ C_{12} &= -2\frac{(s - M_Z^2)c_\theta}{s_\theta s((s - M_Z^2)^2 + M_Z^2\Gamma_Z^2)}, \end{aligned}$$

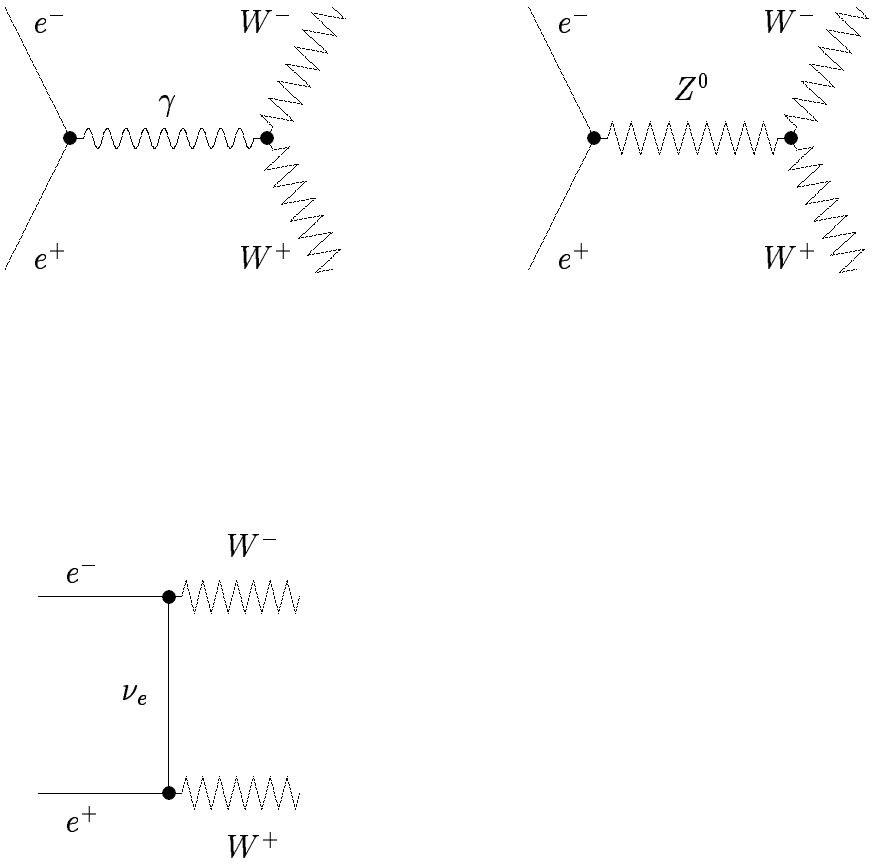

Figure 1: Diagrams contributing to the process $e^+e^- \to W^+W^-$. The full circles represent vertices that include both the lowest order interaction and the anomalous couplings discussed in the text.

$$
\begin{aligned}
C_{22} &= \frac{c_\theta^2}{s_\theta^2((s-M_Z^2)^2+M_Z^2\Gamma_Z^2)}, \\
C_{13} &= \frac{S_2-S_1}{2ss_\theta^2}, \\
C_{23} &= \frac{(s-M_Z^2)c_\theta}{2s_\theta^3((s-M_Z^2)^2+M_Z^2\Gamma_Z^2)}, \\
C_{33} &= \frac{S_1-S_2}{8s_\theta^4},
\end{aligned}
\tag{10}
$$

where S_1 and S_2 carry the dependence on the beam polarization:

$$
S_1 = 1 + z_1 z_2, \quad S_2 = z_1 + z_2 \, . \tag{11}
$$

Analytic expressions for $T_{ij} = T_{ij}(M_W, \kappa_{\gamma,Z}, g_{1\gamma,1Z}, g_5, s, t)$ are given in the Appendix. With θ the angle between the incoming electron and the outgoing W^- in the e^+e^- center of mass frame, we can use Eq. (9) to construct the differential cross-section and the $\cos\theta$ distribution for any angular binning.

3.1 Assumed experimental parameters

In order to study the physics of anomalous couplings at a 500 GeV linear collider, we first need to know some machine and detector parameters.

For the collider we will use an integrated luminosity of $\int \mathcal{L}dt = 50\ fb^{-1}$ per year and a center of mass energy of $\sqrt{s} = 500$ GeV, the numbers commonly used for NLC, CLIC, VLEPP and JLC projects. For the maximal degree of beam polarization we use the values determined by the VLEPP study group [13]: $z_1,\ z_2 = (-0.8,\ 0.8)$. Depending on the mechanism used to polarize the beams it should at least be possible to achieve this high a polarization for the electrons [14]. This is very encouraging because we will find that to place bounds on the anomalous gauge boson couplings of our model there is no need for positron polarization.

We will use the conservative estimates of Ref. [15, 16] for the expected systematic errors in the measurements of the muonic and hadronic cross-sections and asymmetries, and in the luminosity in the experiments at the 500-GeV collider:

	$\Delta\epsilon_\mu/\epsilon_\mu$	$\Delta\epsilon_h/\epsilon_h$	ΔA^l_{FB}	ΔA_{LR}	$\Delta L/L$
Δ_{syst}	0.5%	1.%	$\ll$1.%	0.003	1.%

A detailed investigation of the process $e^+e^- \to W^+W^-$ has shown that the systematic error in the cross-section measurement can be $\sim$2% [17, 18, 19]. This error is due to the uncertainty in the luminosity measurement ($\delta\mathcal{L} \simeq$1%), the error in the acceptance ($\delta_{accep.} \simeq$1%), the error for background subtraction ($\delta_{backgr.} \simeq$0.5%) and a systematic error for the knowledge of the branching ratio ($\delta_{Br} \simeq$0.5%). In order to fully reconstruct the WW-pair events and to identify the W charges, we consider only the "semileptonic" channel, namely, $WW \to l^\pm\nu + 2$-jets. According to the preliminary estimates of Ref. [17, 18], the efficiency for WW-pair reconstruction (using the "semileptonic" channel) is $\epsilon_{WW} = 0.15$. It is easy to estimate that for the anticipated luminosity of $\sim 50\ fb^{-1}$ the expected number of unreconstructed events is $\sim 3.7 \times 10^5$, which corresponds to a relative statistical error in the cross-section value of $\sim 0.17\%$. After reconstruction, the number of WW-pairs is about $\sim 5.5 \times 10^4$, which corresponds to a relative statistical error of $\sim 0.4\%$.

This means that for this process the systematic error may be the dominant one. However, this situation could change when there are kinematical cuts, or when the beams are polarized. To be conservative, we thus include both the statistical error and an estimate of a possible systematic error in our analysis.

3.2 Observables used to bound new physics

The choice of experimental observables and data processing procedure is crucial in analyzing the capability of the future e^+e^- collider to place bounds on new physics. The total and differential cross-sections, as well as the asymmetries of the process under study, are commonly used. To discuss the sensitivity of the $e^+e^- \to W^+W^-$ process to L_{9L}, L_{9R}, and $\hat{\alpha}$, we will use the total cross-section σ_{total} and the asymmetry

A_{FB}. For this process these quantities are defined analogously to the case of $e^+e^- \to f\bar{f}$.[3]

Typically one uses the SM predictions as the "experimental" data,[4] and considers possible effects due to new physics as small deviations. One then requires agreement between the predictions including new physics and the "experimental" values within expected experimental errors. The parameters representing new physics are, thus, bound by requiring that their effect on the selected observables be smaller than the expected experimental errors.

It is common to consider differential distributions such as $d\sigma/d\cos\theta$ as observables (where θ is the angle between the e^--beam direction and the direction of the W^-). However, as it has been emphasized in Ref. [22], it is difficult to perform a meaningful analysis of these distributions in the absence of real experimental data and detailed knowledge of the detector. We start our analysis using the total cross-section and forward-backward asymmetry as observables. These two observables are constructed from the independent measurements of the forward and backward cross-sections σ_F and σ_B. The two observables: $\sigma = \sigma_F + \sigma_B$ and $\sigma \cdot A_{FB} = \sigma_F - \sigma_B$ are thus independent and we can analyze them simultaneously by requiring that:

$$\sqrt{\left(\frac{\sigma - \tilde{\sigma}}{\Delta\sigma}\right)^2 + \left(\frac{A_{FB} - \tilde{A}_{FB}}{\Delta A_{FB}}\right)^2} \leq \text{ number of standard deviations}\,. \qquad (12)$$

In this way we use all the information in the total cross-section, as well as partial information from angular dependence. In Eq. (12) $\sigma \equiv \sigma^{SM}$ and $A_{FB} \equiv A_{FB}^{SM}$ represent anticipated experimental data, $\tilde{\sigma}$ and $\tilde{A}_{FB}$ are the predictions including new physics. $\Delta\sigma$ and ΔA_{FB} are the corresponding absolute uncertainties including systematic and statistical errors.[5] We have:[6]

$$\begin{aligned} \Delta\sigma &= \sigma^{SM} \cdot \sqrt{\delta_{stat}^2 + \delta_{syst}^2}\,, \qquad (13)\\ \delta_{stat} &= \frac{1}{\sqrt{N_{events}}} = \frac{1}{\sqrt{\epsilon_{WW}\mathcal{L}\sigma^{SM}}}\,,\\ \delta_{syst} &= \sqrt{\delta\mathcal{L}^2 + \delta_{accep}^2 + \delta_{backgr}^2 + \delta_{Br}^2}\,, \end{aligned}$$

and

$$\begin{aligned} \Delta A_{FB} &= A_{FB}^{SM} \cdot \sqrt{\delta_{1\,stat}^2 + \delta_{1\,syst}^2}\,, \qquad (14)\\ \delta_{1\,stat} &= \frac{1}{\sqrt{N_{events}}}\sqrt{\frac{1 - A_{FB}^2}{A_{FB}^2}}\,, \end{aligned}$$

[3]Recall that we only use the channel that allows a complete reconstruction of the WW pair.

[4]There are several ways for such data modelling: a) application of the analytical SM expressions to represent "experimental" distributions, see, for example, [19]; b) Monte-Carlo simulation of the experimental distributions according to the SM predictions taking into account a probabilistic spread, see, for example [20, 21].

[5]It should be noted that for the case of A_{FB} the bulk of the systematics (for example the uncertainty due to luminosity measurements), cancels out.

[6]We neglect any correlation between statistical and systematic errors.

$$\delta_{1\,syst} \;=\; \sqrt{\delta^2_{accep} + \delta^2_{backgr} + \delta^2_{Br}}\,,$$

A typical choice for the number of standard deviations in Eq. (12) is two. Assuming a Gaussian distribution for the systematic errors, this 2σ level corresponds to 95% C.L. for the resulting bounds on the parameters under study.

It is possible to use more information from the angular distribution than that present in the forward-backward asymmetry. To do so, one can use a simple χ^2-criterion defined as

$$\chi^2 = \sum_i \left(\frac{X_i - Y_i}{\Delta^i_{exp}} \right)^2 , \tag{15}$$

where

$$X_i = \int_{\cos\theta_i}^{\cos\theta_{i+1}} \frac{d\sigma^{SM}}{d\cos\theta} d\cos\theta, \quad Y_i = \int_{\cos\theta_i}^{\cos\theta_{i+1}} \frac{d\sigma^{NEW}}{d\cos\theta} d\cos\theta\,,$$

and Δ^i_{exp} are the corresponding (expected) experimental errors in each bin defined as in Eq. (13). For the binning we subdivide the chosen range of $\cos\theta$ into equal bins. This procedure gives us a rough idea of the additional information present in the angular distribution. However, a significant analysis of the angular distribution cannot really be done at this stage as discussed in Ref. [22].

3.3 Bounding L_{9L}, L_{9R} and $\hat{\alpha}$

In a scenario for electroweak symmetry breaking like the one discussed in Section 2, we have only three parameters determining the anomalous couplings: L_{9L}, L_{9R}, and $\hat{\alpha}$. This scenario is analyzed in terms of an effective Lagrangian with operators of higher dimension being suppressed by additional powers of the scale of new physics Λ. Our amplitudes involving the couplings L_{9L}, L_{9R} and $\hat{\alpha}$ are, thus, the lowest order terms in a perturbative expansion in powers of $(E^2, v^2)/\Lambda^2$. For the whole formalism to make sense, the corrections to the standard model amplitudes (linear in the anomalous couplings) must be small. For a numerical analysis one can take two different points of view:

- Formally, we have truncated the amplitudes at order $1/\Lambda^2$. Therefore, when calculating the cross-section we must drop the terms quadratic in the anomalous couplings since our calculation is only complete to order $1/\Lambda^2$. We will call this approach the "linear" approximation.

- We may invoke a naturalness assumption, under which we do not expect contributions to an observable that come from different anomalous couplings to cancel each other out. Under this assumption we truncate the amplitudes at order $1/\Lambda^2$, but after this we treat them as exact. We will refer to this approach as the "quadratic" approximation from now on.

Clearly, if the perturbative expansion is adequate, both approaches will lead to the same conclusions; the difference between them being higher order in the $1/\Lambda^2$ expansion. We will mostly use the "linear" approximation, but we will occasionally use

the "quadratic" approximation for comparison as well. Any difference between them may be considered a rough estimate of the theoretical uncertainty.

We will consider three cases: one in which the beams are unpolarized; one in which both electron and positron beams have their maximum degree of polarization, $|z_{e^+,e^-}| = 0.8$; and one in which only the electron beam is polarized, $|z_{e^-}| = 0.8$, $z_{e^+} = 0$.

3.3.1 Dependence on angular cut

The process $e^+e^- \to W^+W^-$ proceeds via the three diagrams in Figure 1. Of these, the t-channel neutrino exchange diagram dominates the cross-section. This dominant contribution to the cross-section, however, does not depend on the new physics parameters L_{9L}, L_{9R}, or $\hat{\alpha}$. Since this dominant contribution is peaked at small values of the angle θ, we expect to improve the sensitivity to new physics by excluding this kinematic region. To implement this idea we impose the cut $|\cos\theta| \leq c < 1$ and study the resulting interplay between a better sensitivity to the anomalous couplings and a loss in the number of events (with the corresponding increase in statistical error). We have studied the dependence of the bounds on the kinematical cut $|\cos\theta| \leq c$ for the range $0.1 \leq c \leq 0.989$ (the upper limit corresponding to the minimal characteristic scattering angle defined by the geometry of the experimental setup [17, 18]). We find that this symmetric kinematical cut does not affect the bounds significantly.

Nevertheless, it is possible to improve the sensitivity of this process to the anomalous couplings by using an *asymmetric* kinematical cut of the form $-1 \leq c_1 \leq \cos\theta \leq c_2 \leq 1$. With a strong cut in the forward direction and a weak cut in the backward hemisphere one can reduce the t-channel background with a tolerable loss of statistics. We have explored the sensitivity of the resulting bounds to the value of the cuts for a wide range of parameters c_1 and c_2, and for different combinations of initial particle polarizations. As a typical example we present in Fig. 2 the allowed $L_{9L} - L_{9R}$ parameter region for unpolarized (dashed line) and maximally polarized (solid line) beams. We set $\hat{\alpha} = 0$, and show three sets of angular cuts for the forward hemisphere: $c_2 = 0.1,\ 0.4,\ 0.989$, while keeping $c_1 = -0.989$. We find an optimal set of cuts that we will use for the remainder of our analysis given by:

$$c_1 = -0.989,\ c_2 \simeq 0.4. \tag{16}$$

3.3.2 Polarization dependence

An interesting question is whether the use of polarized beams significantly improves the bounds that can be placed on the anomalous couplings. A preliminary study in Ref. [11] indicated that the sensitivity to $\hat{\alpha}$ is greatly increased with polarized beams, but only if the degree of polarization is very close to one. Here we study the effect of having a degree of polarization that can be achieved in practice, $z \leq 0.8$.

In Fig. 2b we present the allowed $L_{9L} - L_{9R}$ parameter region (with $\hat{\alpha} = 0$) for maximally ($z_1 = z_2 = 0.8$) polarized and unpolarized beams. We see that the bounds

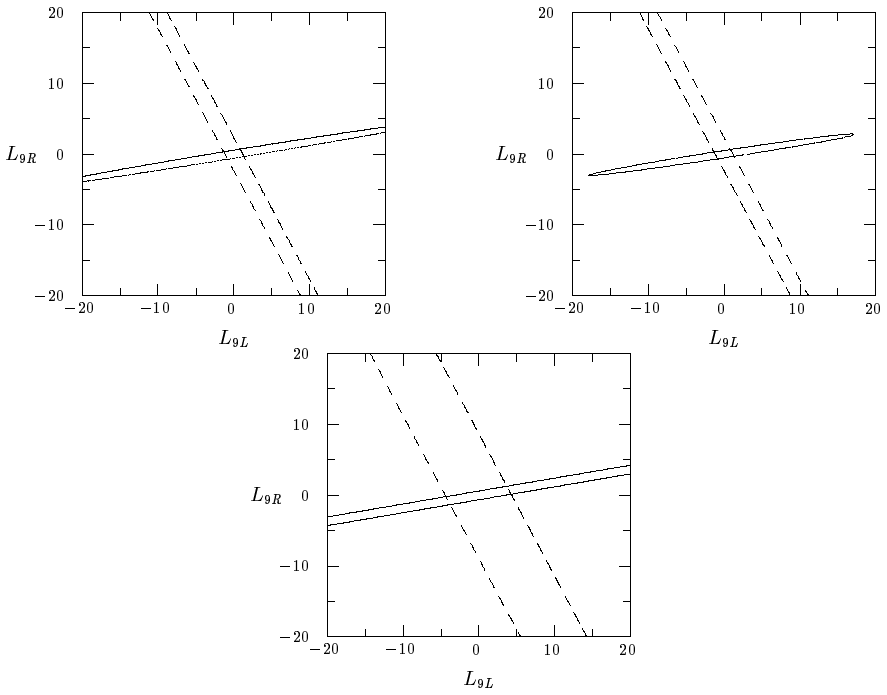

Figure 2: Allowed region for the $L_{9L} - L_{9R}$ parameters at $\hat{\alpha} = 0$ for the initial beam polarizations $z_1 = z_2 = 0.8$ (solid contour) and $z_1 = z_2 = 0$ (dashed contour) for cuts on the scattering angle $-0.989 \leq \cos\theta \leq c_2$, where: a) $c_2 = 0.1$; b) $c_2 = 0.4$; c)$c_2 = 0.989$. We use the "linear" approximation discussed in the text.

that can be obtained with polarized beams (solid lines) are slightly better than the bounds that can be obtained with unpolarized beams (dashed lines). This effect is due to the reduction of the relative contribution of the "background" t-channel diagram which results in a better sensitivity of the process to the anomalous couplings. With the maximum degree of polarization that can be achieved in practice, one does not find the spectacular effects that could be found with completely polarized beams [11].

Nevertheless, polarized beams are very useful to constrain new physics that is described by several unknown parameters. The unpolarized case can only constrain a particular linear combination of parameters (in this case L_{9L} and L_{9R}) thus giving the dashed band shown in Fig. 2b. The polarized result depends on a *different* linear combination of parameters. The simultaneous study of polarized and unpolarized collisions can, therefore, give much better bounds on the anomalous couplings than either one of them separately.

An intermediate degree of polarization, such as $z_1 = z_2 = 0.4$ also leads to an improvement of the bounds (see Fig. 3a), although it is not as effective as the case with maximum practical degree of polarization in reducing the allowed region of parameter space when combined with the unpolarized measurement. If polarization is available only for the electron beam it is still possible to reduce the region of parameter space that is allowed by the unpolarized measurement. We illustrate this

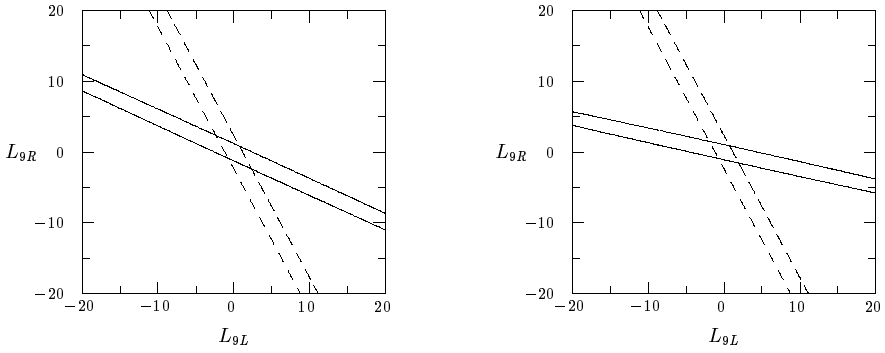

Figure 3: Allowed region for the $L_{9L} - L_{9R}$ parameters at $\hat{\alpha} = 0$ for cuts on the scattering angle $-0.989 \leq \cos\theta \leq 0.4$ for beam polarizations (dashed contour represents the unpolarized case): a) $z_1 = z_2 = 0.4$; b) $z_1 = 0.8$, $z_2 = 0$. We use the "linear" approximation discussed in the text.

in Fig. 3b where we show the case $z_1 = 0.8$, $z_2 = 0$.

Using the "quadratic" approximation, one finds that each allowed region of parameter space in Fig. 3 is replaced by several possible regions. This is because the terms that are quadratic in the anomalous couplings in the cross-section give rise to allowed regions shaped like ellipsoids. The case with polarized beams gives rise to a rotated ellipsoid, and the two intersect in more than one region. It is obvious, however, that only the region that contains the standard model point is physical, and this region is very much like that shown in Fig. 3 for the "linear" approximation. It is interesting to notice that one could decide which is the true allowed region experimentally. By changing the degree of polarization one obtains a different rotated ellipsoid that intersects the unpolarized one in several regions. Only the region containing the standard model point is common to the different degrees of beam polarization. This further illustrates the complementarity of polarized and unpolarized measurements.

4 Results

We first present the bounds on the anomalous couplings that follow from Eq. (12). In the case of the "quadratic" approximation, the cross-section contains terms that are quadratic in the anomalous couplings, as well as interference terms between the different anomalous couplings. The allowed parameter region is a volume element in the $L_{9L} - L_{9R} - \hat{\alpha}$ space enclosed by a nontrivial surface. Due to the interplay between couplings, the allowed volume may have holes, and therefore, it is in general not adequate to study two dimensional projections. In keeping with our previous discussion we select the allowed region that contains the standard model point, and that is very similar in shape to the results of the "linear" approximation. Doing this we have a simple region for which two-dimensional projections are adequate.

We present in Fig. 4 the two-dimensional projections obtained in the directions in which one of the three anomalous couplings vanishes. We present the case corre-

sponding to two standard deviation (95% C.L.) bounds from Eq. (12). These results correspond to the "linear" approximation, but are practically identical to those obtained in the "quadratic" approximation. Thus, the bounds correspond to anomalous couplings that are small enough for the perturbative expansion to be meaningful. This, in itself, indicates that a 500 GeV linear collider with polarized beams will be able to place significant bounds on a strongly interacting symmetry breaking sector. Allowing two of the couplings to vary and setting the third one to its standard model value we find ("linear" case):

$$\begin{aligned} -1.4 \leq \quad & L_{9L} \quad \leq 1.4\,, \\ -0.7 \leq \quad & L_{9R} \quad \leq 0.7\,, \\ -3.3 \leq \quad & \hat{\alpha} \quad \leq 3.3\,. \end{aligned} \tag{17}$$

or ("quadratic" case):

$$\begin{aligned} -1.3 \leq \quad & L_{9L} \quad \leq 1.3\,, \\ -0.6 \leq \quad & L_{9R} \quad \leq 0.7\,, \\ -3.4 \leq \quad & \hat{\alpha} \quad \leq 3.2\,. \end{aligned} \tag{18}$$

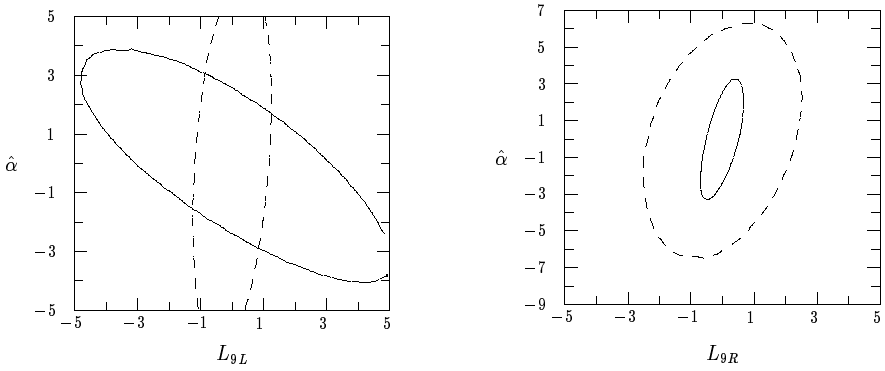

Figure 4: Allowed regions (the case of the linear approximation) for: a) $L_{9L} - \hat{\alpha}$, when $L_{9R} = 0$; b) $L_{9R} - \hat{\alpha}$, when $L_{9L} = 0$. The solid contours correspond to the maximum beam polarization $z_1 = z_2 = 0.8$ and the dashed contours correspond to unpolarized beams.

It is worth mentioning that the allowed regions are sometimes bound by curved lines, even in the "linear" approximation. This is due to the intrinsically non-linear combination of observables that we used, Eq. (12). In this respect, one interesting feature can be seen in Fig. 4. While the allowed regions in Fig. 4a and Fig. 4b are bounded by curves, the domain in Fig. 2b is bound by almost straight lines. This means that the deviations of the L_{9L}, L_{9R} parameters affect mainly the cross-section, but practically do not modify the forward-backward asymmetry. In terms of the angular distribution this can be rephrased saying that variations of the couplings L_{9L}, L_{9R} lead to a change of the overall normalization of the differential cross-section, while changes in $\hat{\alpha}$ lead to changes in the shape of the distribution. This effect will be demonstrated further when we discuss the angular distributions.

4.1 χ^2 Analysis of the Angular Distribution

In this section we discuss the bounds on the anomalous couplings that can be obtained from the analysis of the differential cross-section $d\sigma/d\cos\theta$. We will use the χ^2 criterion in the form of Eq. (15) with experimental uncertainties defined in Eq. (13). We will allow two parameters to vary at a time while fixing the third one at its standard model value (0 at tree-level). Therefore, in order to use a χ^2 approach we need a minimum of 4 bins to have $N_{DOF} = N_{measurements} - N_{parameters} - 1 = 1$. We will consider the cases with the angular region $(-0.989 < \cos\theta < 0.4)$ divided into 4, 5, and 10 bins. To compare these χ^2 results with those obtained in the previous section using the criterion Eq. (12), we adopt the same C.L. of 95%.

For the χ^2 approach it is important to understand which is the number of bins that gives the strongest bounds on the parameters given an event sample. As we mentioned before, the total expected number of reconstructed WW-events for the chosen luminosity is $\sim 5.5 \times 10^4$. However, with the kinematical cut on scattering angle that we use, $-0.989 < \cos\theta < 0.4$, this number is reduced to 4384 events. With unpolarized beams and choosing 4 angular bins, the number of events in each bin varies from 327 to 2175 (with the smaller number in the backward-most bin). These numbers correspond to relative statistical errors varying from 3.8% to 2.1%. For the case of 5(10) bins the number of events varies from 229(81) to 1854(1068), and the statistical error varies from 6.6%(11.1%) to 2.3%(3.1%). If the beams are polarized there is an even larger loss of statistics due to the partial cancellation of the dominant t-channel diagram. One can see that for these binnings of the events the corresponding statistical errors are larger than the systematic error. This means that we have a statistically unsaturated event sample, and the strongest bounds are obtained with the minimum number of bins.

Before using the angular distribution to place bounds on the parameters, it is useful to see the behaviour of this distribution for small deviations from the standard model. For illustration purposes we choose the values $L_{9L} = 5$, $L_{9R} = 5$, and $\hat{\alpha} = 5$. Notice that these numbers are are small enough to neglect the difference between the "quadratic" and "linear" approximations.

In Fig. 5 we show the behaviour of the angular distribution for the unpolarized case in the range $-0.989 < \cos\theta < 0.4$, normalized to the angular distribution predicted by the standard model. The solid line corresponds to $L_{9L} = 5$, the short dashed line corresponds to $L_{9R} = 5$, and the long dashed line corresponds to $\hat{\alpha} = 5$. In Fig. 5a (5b) we present the normalized angular distributions for unpolarized (polarized) beams. One can see in Fig. 5a that variations of L_{9L} and L_{9R} lead to a change in the overall normalization of the distribution; whereas variations in $\hat{\alpha}$ result in a change in the shape of the distribution. However, this difference is not evident in the case of polarized beams (see Fig. 5b).

In Fig. 6 we show the projection of the allowed parameter region in the $L_{9L} - L_{9R}$ plane for unpolarized beams, which corresponds to 95% C.L. in the χ^2-analysis for the cases of 4 (solid line), 5 (short-dashed line), and 10 (long-dashed line) bins. One can see that the best bounds are, indeed, obtained with the smallest number of bins,

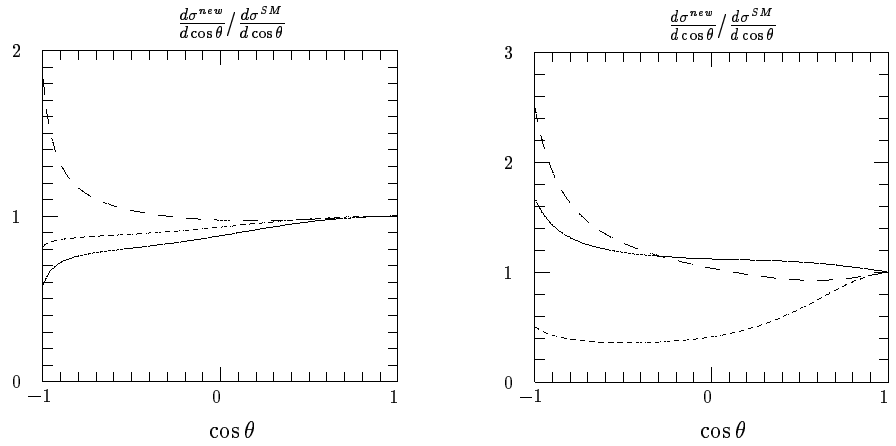

Figure 5: Angular distributions normalized to the standard model for a) unpolarized beams ($z_1 = z_1 = 0.0$) and b) maximally polarized beams ($z_1 = z_1 = 0.8$). The solid, short-dashed and long-dashed lines correspond to $L_{9L} = 5$, $L_{9R} = 5$, and $\hat{\alpha} = 5$ respectively.

four. The same result holds true for polarized beams.

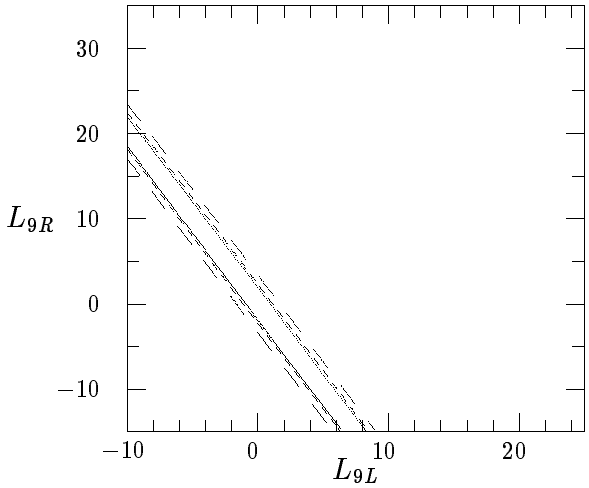

Figure 6: $L_{9L} - L_{9R}$-projections of the allowed parameter region ("linear" approximation) for the unpolarized case ($z_1 = z_2 = 0.0$) corresponding to a 95% C.L. χ^2-analysis for the cases of 4 (solid line), 5 (short-dashed line), and 10 (long-dashed line) bins.

We find that the angular distribution gives slightly better bounds than the combined criterion of Eq. (12), as shown in Fig. 7.

Thus, choosing the case of 4 bins we can present the resulting bounds on L_{9L}, L_{9R}, and $\hat{\alpha}$ following from the χ^2-analysis of the angular distribution, which are shown in Fig. 7. The two-parameter fit bounds (setting one of the three couplings at a time to its standard model value) are:

$$-1.2 \;\leq\; L_{9L} \;\leq\; 1.0\,,$$

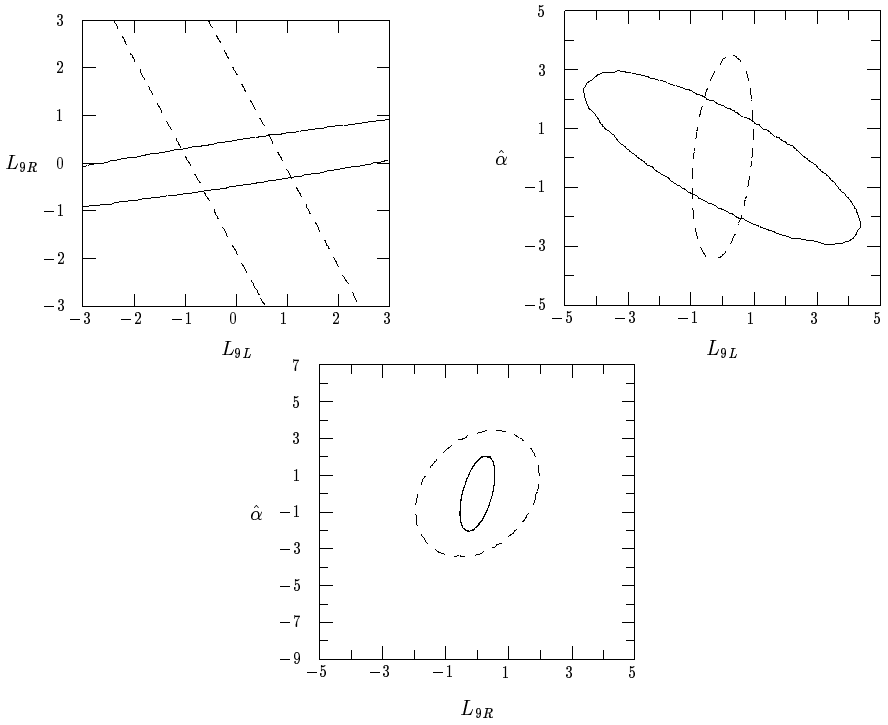

Figure 7: Allowed regions ("linear" approximation) from a χ^2 analysis with four bins. The dashed curves correspond to $z_1 = z_2 = 0$ and the solid curves to $z_1 = z_2 = 0.8$. a) $L_{9L} - L_{9R}$, when $\hat{\alpha} = 0$; b) $L_{9L} - \hat{\alpha}$, when $L_{9R} = 0$; c) $L_{9R} - \hat{\alpha}$, when $L_{9L} = 0$.

$$\begin{aligned} -0.6 \;\leq\; & L_{9R} \;\leq\; 0.7\,, \\ -3.5 \;\leq\; & \hat{\alpha} \;\leq\; 3.5\,. \end{aligned} \tag{19}$$

5 Summary and Conclusions

If the electroweak symmetry breaking sector is strongly interacting, and there are no new resonances below a TeV one expects deviations of the gauge boson self-interactions from their standard model values. In theories that conserve CP and have an approximate custodial symmetry we can parameterize these deviations in terms of three constants, L_{9L}, L_{9R} and $\hat{\alpha}$. An e^+e^- collider operating at $\sqrt{s} = 0.5$ TeV with polarized beams and an integrated luminosity of 50 fb^{-1} can provide important input into our understanding of the nature of electroweak symmetry breaking. We find that such a collider can place the following bounds:

$$\begin{aligned} (-1.4 \to -1.2) \;\leq\; & L_{9L} \;\leq\; (1.0 \to 1.4)\,, \\ (-0.7 \to -0.6) \;\leq\; & L_{9R} \;\leq\; 0.7\,, \\ (-3.5 \to -3.3) \;\leq\; & \hat{\alpha} \;\leq\; (3.2 \to 3.5)\,. \end{aligned} \tag{20}$$

The ranges correspond to the difference between the "linear" and "quadratic" approximations, and to the difference between using the simple criterion of Eq. (12) and a

more sophisticated χ^2 analysis of the angular distribution. These differences can be taken as a rough guide of the theoretical uncertainties under our stated assumptions.

The authors of Ref.[18] have also studied the process $e^+e^- \to W^+W^-$ in terms of anomalous couplings at a future e^+e^- collider like the one we discuss here. Because they do not have in mind a strongly interacting electroweak symmetry breaking sector, as we do, they look for deviations of the standard model in terms of a larger number of parameters than we do. They do not, however, study the parity violating coupling $\hat{\alpha}$. A meaningful comparison of their results with ours involves their two-parameter fit to their quantities δ_Z and X_γ which we translate into[7]

$$\begin{aligned} -2.0 \;\leq\; & L_{9L} \;\leq 1.8\,, \\ -3.4 \;\leq\; & L_{9R} \;\leq 4.7\,, \end{aligned} \tag{21}$$

We can see that the bounds we obtained by combining unpolarized and polarized collisions are significantly better. This is especially true for the case of L_{9R}. This emphasizes the additional sensitivity to new physics provided by polarized beams.

We have shown that polarized beams with adjustable degrees of polarization would constitute a very significant tool in the search for new physics. In terms of new physics parameterized by a set of anomalous couplings, beam polarization makes it possible to explore directions of parameter space that cannot be reached in unpolarized collisions.

To place our bounds in perspective, we now compare them to those obtained from LEP I and those that can be obtained at LEP II. Precision measurements of Z partial widths imply [12]:

$$\begin{aligned} -28 \;\leq\; & L_{9L} \;\leq 27\,, \\ -9 \;\leq\; & \hat{\alpha} \;\leq 5\,, \\ -100 \;\leq\; & L_{9R} \;\leq 190\,. \end{aligned} \tag{22}$$

Expected bounds from LEP II with $\sqrt{s} = 190$ GeV and $\int \mathcal{L}dt = 500$ pb^{-1} are [2]

$$\begin{aligned} -41 \;\leq\; & L_{9L} \;\leq 26\,, \\ -100 \;\leq\; & L_{9R} \;\leq 330\,. \end{aligned} \tag{23}$$

Similar bounds have been obtained for different future colliders. For example, with an $e\gamma$-collider with $\sqrt{s_{ee}} = 500$ GeV and $\int \mathcal{L}dt = 50$ fb^{-1} they are [10]:

$$\begin{aligned} (-7 \to -5) \;\leq\; & L_{9L} \;\leq (4 \to 6)\,, \\ (-17 \to -5) \;\leq\; & L_{9R} \;\leq (4 \to 16)\,, \\ -15 \;\leq\; & \hat{\alpha} \;\leq 7\,. \end{aligned} \tag{24}$$

Studies for the LHC (with $\sqrt{s} = 14$ TeV and integrated luminosity 100 fb^{-1}) have found [3] a sensitivity to L_{9L} of order 10.

[7] Our χ^2 analysis is different from that of Ref. [18], page 747. Nevertheless, we take their results at face value to compare with our results since their bounds would be weaker using our χ^2 criterion and our conclusion remains the same.

After completion of this paper a similar analysis by M. Ginter *et. al.* has appeared [23]. These authors consider polarized electron beams as we do, and they reach similar conclusions to ours for the parameters that are common to our study[8] in the case of one-parameter fits.

Acknowledgements

The work of A. A. L. has been made possible by a fellowship of Royal Swedish Academy of Sciences and is carried out under the research program of International Center for Fundamental Physics in Moscow. A. A. L.is also supported in part by the International Science Foundation under grants NJQ000 and NJQ300. The work of T.H. is supported in part by the DOE grant DE-FG03-91ER40674 and in part by a UC-Davis Faculty Research Grant. The work of G.V. was supported in part by the DOE OJI program under contract number DE-FG02-92ER40730. We thank S. Dawson for useful discussions.

Analytic expressions for the cross-section

We present below the explicit expressions for the dimensional functions $T_{ij} = T_{ij}(M_W,\, \kappa_{\gamma,Z}, g_{1\gamma,1Z},\, g_5,\, s,\, t)$ used in expressions (9) for the cross-section of the $e^+e^- \to W^+W^-$ process. In this appendix we use $M \equiv M_W$, and t is the absolute value of the usual Mandelstam variable. Because we do not need to consider the renormalization due to L_{10} as explained in the text, the parameters $a_f = T_{3f}/2c_\theta s_\theta$ and $v_f = (T_{3f} - 2Q_f s_\theta^2)/2s_\theta c_\theta$ are the usual tree-level standard-model axial and vector couplings of the Z to fermions.

$$
\begin{aligned}
T_{11} = \frac{t^3}{3} \;&\cdot\; (4sM^2g_{1\gamma}^2 + 4sM^2\kappa_\gamma^2 - 24M^4g_{1\gamma}^2 - 2s^2\kappa_\gamma^2) \\
-\frac{t^2}{2} \;&\cdot\; (4s^2M^2g_{1\gamma}^2 + 8s^2M^2\kappa_\gamma^2 - 32sM^4g_{1\gamma}^2 - 8sM^4\kappa_\gamma^2 + 48M^6g_{1\gamma}^2 - 2s^3\kappa_\gamma^2) \\
+t \;&\cdot\; (4s^3M^2g_{1\gamma}\kappa_\gamma + 2s^3M^2g_{1\gamma}^2 + 2s^3M^2\kappa_\gamma^2 - 16s^2M^4g_{1\gamma}^2\kappa_\gamma - 8s^2M^4g_{1\gamma}^2 \\
&\quad -10s^2M^4\kappa_\gamma^2 + 4sM^6g_{1\gamma}^2 + 4sM^6\kappa_\gamma^2 - 24M^8g_{1\gamma}^2)
\end{aligned}
$$

$$
\begin{aligned}
T_{12} = \frac{t^3(v_eS_1 - a_eS_2)}{3} \;&\cdot\; (4sM^2g_{1Z}g_{1\gamma} + 4sM^2\kappa_Z\kappa_\gamma - 24M^4g_{1Z}g_{1\gamma} - 2s^2\kappa_Z\kappa_\gamma) \\
-\frac{t^2(v_eS_1 - a_eS_2)}{2} \;&\cdot\; (4s^2M^2g_{1Z}g_{1\gamma} + 8s^2M^2\kappa_Z\kappa_\gamma - 32sM^4g_{1Z}g_{1\gamma} - 8sM^4\kappa_Z\kappa_\gamma \\
&\quad +48M^6g_{1Z}g_{1\gamma} - 2s^3\kappa_Z\kappa_\gamma)
\end{aligned}
$$

[8] These are L_{9L} and L_{9R} albeit with a different normalization.

$$
\begin{aligned}
+t(v_eS_1 - a_eS_2) \quad &\cdot \quad (2s^3M^2g_{1Z}g_{1\gamma} + 2s^3M^2g_{1Z}\kappa_\gamma + 2s^3M^2\kappa_Z g_{1\gamma} + 2s^3M^2\kappa_Z\kappa_\gamma \\
&\quad -8s^2M^4g_{1Z}g_{1\gamma} - 8s^2M^4g_{1Z}\kappa_\gamma - 8s^2M^4\kappa_Z g_{1\gamma} - 10s^2M^4\kappa_Z\kappa_\gamma \\
&\quad +4sM^6g_{1Z}g_{1\gamma} + 4sM^6\kappa_Z\kappa_\gamma - 24M^8g_{1Z}g_{1\gamma}) \\
-\frac{t^2(a_eS_1 - v_eS_2)g_5}{2} \quad &\cdot \quad (4s^2M^2g_{1\gamma} + 4s^2M^2\kappa_\gamma - 16sM^4g_{1\gamma} - 16sM^4\kappa_\gamma) \\
+t(a_eS_1 - v_eS_2)g_5 \quad &\cdot \quad (2s^3M^2g_{1\gamma} + 2s^3M^2\kappa_\gamma - 12s^2M^4g_{1\gamma} - 12s^2M^4\kappa_\gamma + 16sM^6g_{1\gamma} \\
&\quad +16sM^6\kappa_\gamma)
\end{aligned}
$$

$$
\begin{aligned}
T_{13} = \frac{t^3}{3} \quad &\cdot \quad (4M^2g_{1\gamma} - 2s\kappa_\gamma) \\
-\frac{t^2}{2} \quad &\cdot \quad (4sM^2g_{1\gamma} + 4sM^2\kappa_\gamma - 2s^2\kappa_\gamma) \\
+t \quad &\cdot \quad (4s^2M^2g_{1\gamma} + 4s^2M^2\kappa_\gamma - 10sM^4\kappa_\gamma - 12M^6g_{1\gamma}) \\
-\ln\Big(\frac{t}{1\ \mathrm{GeV}^2}\Big) \quad &\cdot \quad (8sM^6g_{1\gamma} + 8sM^6\kappa_\gamma + 8M^8g_{1\gamma})
\end{aligned}
$$

$$
\begin{aligned}
T_{22} = \frac{t^3((v_e^2+a_e^2)S_1 - 2v_ea_eS_2)}{3} \quad &\cdot \quad (4sM^2g_{1Z}^2 + 4sM^2\kappa_Z^2 - 24M^4g_{1Z}^2 - 2s^2\kappa_Z^2) \\
-\frac{t^2((v_e^2+a_e^2)S_1 - 2v_ea_eS_2)}{2} \quad &\cdot \quad (4s^2M^2g_{1Z}^2 + 8s^2M^2\kappa_Z^2 - 32sM^4g_{1Z}^2 - 8sM^4\kappa_Z^2 \\
&\quad +48M^6g_{1Z}^2 - 2s^3\kappa_Z^2) \\
+t((v_e^2+a_e^2)S_1 - 2v_ea_eS_2) \quad &\cdot \quad (4s^3M^2g_{1Z}\kappa_Z + 2s^3M^2g_{1Z}^2 + 2s^3M^2\kappa_Z^2 \\
&\quad -16s^2M^4g_{1Z}\kappa_Z - 8s^2M^4g_{1Z}^2 - 10s^2M^4\kappa_Z^2 + 4sM^6g_{1Z}^2 \\
&\quad +4sM^6\kappa_Z^2 - 24M^8g_{1Z}^2) \\
-\frac{t^2g_5(2v_ea_eS_1 - (v_e^2+a_e^2)S_2)}{2} \quad &\cdot \quad (8s^2M^2g_{1Z} + 8s^2M^2\kappa_Z - 32sM^4g_{1Z} - 32sM^4\kappa_Z) \\
+tg_5(2v_ea_eS_1 - (v_e^2+a_e^2)S_2) \quad &\cdot \quad (4s^3M^2g_{1Z} + 4s^3M^2\kappa_Z - 24s^2M^4g_{1Z} - 24s^2M^4\kappa_Z \\
&\quad +32sM^6g_{1Z} + 32sM^6\kappa_Z) \\
+\frac{t^3g_5^2((v_e^2+a_e^2)S_1 - 2v_ea_eS_2)}{3} \quad &\cdot \quad (4sM^2 - 16M^4) \\
-\frac{t^2g_5^2((v_e^2+a_e^2)S_1 - 2v_ea_eS_2)}{2} \quad &\cdot \quad (4s^2M^2 - 24sM^4 + 32M^6) \\
+tg_5^2((v_e^2+a_e^2)S_1 - 2v_ea_eS_2) \quad &\cdot \quad (2s^3M^2 - 16s^2M^4 + 36sM^6 - 16M^8)
\end{aligned}
$$

$$
\begin{aligned}
T_{23} = \frac{t^3}{3} \quad &\cdot \quad (4M^2g_{1Z} - 2s\kappa_Z) \\
-\frac{t^2}{2} \quad &\cdot \quad (4sM^2\kappa_Z + 4sM^2g_{1Z} - 2s^2\kappa_Z)
\end{aligned}
$$

$$
\begin{aligned}
+t &\cdot (4s^2M^2\kappa_Z + 4s^2M^2 g_{1Z} - 10sM^4\kappa_Z - 12M^6 g_{1Z}) \\
-\ln\!\left(\frac{t}{1\ \mathrm{GeV}^2}\right) &\cdot (8sM^6\kappa_Z + 8sM^6 g_{1Z} + 8M^8 g_{1Z}) \\
-\frac{t^2 g_5}{2} &\cdot (8sM^2 - 8M^4) \\
+t g_5 &\cdot (4s^2M^2 - 8sM^4 + 16M^6) \\
-\ln\!\left(\frac{t}{1\ \mathrm{GeV}^2}\right) g_5 &\cdot (8sM^6 - 8M^8)
\end{aligned}
$$

$$
T_{33} = -\frac{2}{3}t^3 - \frac{1}{2}t^2(4M^2 - 2s) + t(8sM^2 - 10M^4) - \ln\!\left(\frac{t}{1\ \mathrm{GeV}^2}\right)(-8sM^4 + 16M^6) + \frac{8}{t}M^8
$$

References

[1] See for example P. B. Renton, Plenary talk at LP95, Beijing, August 1995.

[2] F. Boudjema, in proceedings of *Physics and Experiments with Linear e^+e^- Colliders*, ed. by F. A. Harris *et al.*, (1993), p. 713, and references therein.

[3] H. Aihara, *et. al.*, DPF Anomalous Gauge Boson Interaction Subgroup Report, hep-ph/9503425.

[4] J. Bagger, S. Dawson and G. Valencia, *Nucl. Phys.* **B399** 364 (1993).

[5] T. Appelquist and C. Bernard, *Phys. Rev.* **D22** 200 (1980); A. Longhitano, *Nucl. Phys.* **B188** 118 (1981).

[6] B. Holdom, *Phys. Lett.* **258B** 156 (1991).

[7] A. Falk, M. Luke, and E. Simmons, *Nucl. Phys.* **B365** 523 (1991).

[8] T. Appelquist and G.-H. Wu, *Phys. Rev.* **D48** 3235 (1993).

[9] K. Hagiwara *et. al.*, *Nucl. Phys.* **B282** 253 (1987).

[10] Kingman Cheung, *et. al.*, *Phys. Rev.* **D51** 5 (1995).

[11] S. Dawson and G. Valencia, *Phys. Rev.* **D49** 2188 (1994).

[12] S. Dawson and G. Valencia, *Nucl. Phys.* **B439** 3 (1995); S. Dawson and G. Valencia, *Phys. Lett.* **B333** 207 (1994).

[13] S. Ecklund, in proceedings of *Third International Workshop on Linear Colliders*, LC91, ed. by V.Balakin *et. al.*, September 17-27, BINP, Protvino, Russia, v.2, p.197 (1991); R. Chebab, *ibid.*; The possibility of having polarized positron beams is discussed by A. Mikhailichenko, *ibid.* p.247.

[14] C. Prescott, in proceedings of *Workshop on Physics and Experiments with Linear e^+e^- Colliders*, ed. by F. A. Harris *et. al.*, p. 379.

[15] A. Djouadi *et. al.*, in proceedings of *Workshop on Physics and Experiments with Linear Colliders*, Saariselka, Finland, 515 (1991); A. Djouadi *et. al.*, *Z. Phys.* **C56** 289 (1992).

[16] D. J. Miller, in proceedings of *Workshop on "e^+e^- at 500 GeV: the Physics Potential"*, ed. P. Zerwas DESY Hamburg (1991).

[17] M. Frank et al., in proceedings of *Workshop " e^+e^- collisions at 500 GeV: the Physics Potential"*, ed. P.M.Zerwas DESY Hamburg, 223 (1991).

[18] G. Gounaris et al., in proceedings of *Workshop " e^+e^- collisions at 500 GeV: the Physics Potential"*, ed. P.M.Zerwas DESY Hamburg, 735 (1991).

[19] S. Y. Choi and F. Schrempp, *Phys. Lett.* **B272** 149 (1991).

[20] A. Miyamoto, in proceedings of the 2nd *Workshop on Jap. LinearCollider (JLC)*, Tsukuba Japan, p.256 (1990).

[21] T. Barklow, in proceedings of *Workshop on Physics and Experiments with Linear Colliders*, Saariselka, Finland, 423 (1991).

[22] A. A. Likhoded et al., *Sov. Journ. Nucl. Phys.* **58** (1995) 56.

[23] M. Ginter, S. Godfrey and G. Couture, hep-ph/9511204, OCIP/C 95-3, UQAM-PHE-95-08.